

Rouse Dynamics of Polyelectrolyte Solutions: Molecular Dynamics Study

Qi Liao,[†] Jan-Michael Y. Carrillo,[‡] Andrey V. Dobrynin,^{*,‡} and Michael Rubinstein[§]

State Key Laboratory of Polymer Physics and Chemistry, Joint Laboratory of Polymer Science and Materials, Institute of Chemistry, Chinese Academy of Sciences, Beijing, 100080, China, Polymer Program, Institute of Materials Science and Department of Physics, University of Connecticut, Storrs, Connecticut, 06269-3136, and Department of Chemistry, University of North Carolina, Chapel Hill, North Carolina 27599-3290

Received March 19, 2007; Revised Manuscript Received July 27, 2007

ABSTRACT: We performed molecular dynamics simulations of dilute and semidilute polyelectrolyte solutions without hydrodynamic interactions to study Rouse dynamics of polyelectrolytes. Polyelectrolyte solutions are modeled by an ensemble of bead–spring chains of charged Lennard-Jones particles with explicit counterions. The simulations were performed for partially and fully charged polymers with the number of monomers $N = 25–373$. We show that the simulations of the Rouse dynamics give qualitatively similar results to the experimentally observed dynamics of polyelectrolyte solutions. Our simulations showed that the chain relaxation time depends nonmonotonically on polymer concentration. In dilute solutions, this relaxation time exhibits very strong dependence on the chain degree of polymerization, $\tau \sim N^3$. The chain relaxation time decreases with increasing polymer concentration of dilute solutions. This decrease in the chain relaxation time is due to chain contraction induced by counterion condensation. In the semidilute solution regime the chain relaxation time decreases with polymer concentration as $c^{-1/2}$. In this concentration range the chain relaxation time follows the usual Rouse scaling dependence on the chain degree of polymerization, $\tau \sim N^2$. At high polymer concentrations the chain relaxation time begins to increase with increasing polymer concentration. The crossover polymer concentration to the new scaling regime does not depend on the chain degree of polymerization, indicating that the increase in the chain relaxation time is due to the increase of the effective monomeric friction coefficient. The analysis of the spectrum and of the relaxation times of Rouse modes confirms the existence of the single correlation length ξ , which describes both static and dynamic properties of semidilute solutions.

1. Introduction

Polyelectrolytes are polymers with ionizable groups. Examples of charged polymers include biopolymers such as DNA and RNA, and synthetic polymers such as poly(styrene-sulfonate), poly(acrylic acids), and poly(methacrylic acids). In polar solvents, these groups dissociate releasing counterions and leaving uncompensated charges on the polymer backbones. The presence of the long-range electrostatic interactions between ionized groups results in unique dynamic properties of polyelectrolyte solutions that are qualitatively different from their neutral counterparts.^{1–6}

The well-known feature of polyelectrolyte solutions is the concentration dependence of the solution viscosity called the Fuoss law (see, for review, ref 2). The viscosity of polyelectrolyte solutions is proportional to the square root of polymer concentration in the wide concentration range, while the viscosity of uncharged polymers in a good solvent scales linearly with polymer concentration in a dilute solution regime or as $c^{1.3}$ in a semidilute solution regime. Furthermore, in this concentration range the chain relaxation time decreases with increasing polymer concentration indicating that the stress relaxation in polyelectrolyte solutions speeds up as they become denser. The physical origin of this unique behavior is the

coupling of electrostatic interactions with conformational transformations of charged macromolecules. The unusually wide Fuoss law regime supports the conjecture that the entanglements (topological constraints created by surrounding chains)⁷ in polyelectrolyte solutions begin to restrict chain motion deep in the semidilute solution regime. The crossover to entangled polyelectrolyte solutions occurs 3–4 decades above the overlap concentration c^* .^{8,9} Note that in solutions of neutral polymers this crossover takes place closer to the chain overlap concentration at approximately $10c^*$.

The modern theories of polyelectrolyte dynamics were successful in explaining the origin of the unusual dynamic properties of polyelectrolyte solutions.^{2,8,10–12} Unfortunately, experimental data^{13,14–23} alone cannot provide a detailed test of the microscopic foundations of these models. Computer simulations^{24–31} play an important role in our understanding the static properties of polyelectrolyte solutions by providing a valuable insight into molecular origin of the phenomena and by direct testing the assumptions of the theoretical models. Understanding of molecular processes controlling dynamics of polyelectrolyte solutions, e.g., flow properties of DNA solutions in microfluidic devices, dynamics of spreading of polyelectrolyte solutions over surfaces, kinetics of assembly of multilayered polyelectrolyte thin films^{2,5,32,33} will have far reaching consequences in different branches of natural sciences ranging from biophysics to materials science and nanotechnology.

In this paper, we present results of a computer simulation study of the polyelectrolyte solution dynamics. Our molecular dynamics simulations correspond to the free draining (Rouse) dynamics^{7,34,35} of the polyelectrolyte solutions. We demonstrate

* Corresponding authors. E-mail (A.V.D.): avd@ims.uconn.edu.

[†] State Key Laboratory of Polymer Physics and Chemistry, Joint Laboratory of Polymer Science and Materials, Institute of Chemistry, Chinese Academy of Sciences.

[‡] Polymer Program, Institute of Materials Science and Department of Physics, University of Connecticut

[§] Department of Chemistry, University of North Carolina, Chapel Hill.

that the Rouse model of polyelectrolytes is useful for understanding the dynamics of real polyelectrolyte solutions. In real solutions, there is strong hydrodynamic coupling between sections of moving object due to hydrodynamics interactions on the length scales shorter than hydrodynamic screening length. For a fractal object consisting of N monomeric units and having size $R \sim N^\nu$, where $1/\nu$ is the object's fractal dimension, the characteristic Zimm relaxation time scales with the object size, R , and number, N , of monomers in it as $\tau_Z \propto R^3 \approx N^{3\nu}$. The Rouse relaxation time of a similar object⁷ is $\tau_R \propto R^2 N \approx N^{2\nu+1}$. By comparing the expressions for Zimm and Rouse relaxation times, one can immediately see that they are proportional to each other when the fractal dimension of the object is one, $\nu = 1$, which corresponds to a rodlike object. This is indeed the case for a polyelectrolyte chain in a dilute solution. (Note that there are additional logarithmic corrections to the N -scaling of relaxation time appearing in the relaxation time of a rod as well as due to nonuniform stretching of a polyelectrolyte chain.^{2,30}) The similarities between Rouse and Zimm models of a polyelectrolyte chain is due to the fact that both electrostatic and hydrodynamic interactions are long-range which is manifested in strong coupling between monomer motion. It turns out that the incorporation of electrostatic interactions into Rouse dynamics provides qualitatively correct description of the chain relaxation. The addition of hydrodynamic interactions will not lead to qualitatively new results but rather to logarithmic corrections to the Rouse model. This is a unique feature of polyelectrolyte solutions.

In the following sections, we present scaling analysis of the Rouse dynamics in dilute and semidilute polyelectrolyte solutions and compare its predictions with the results of our molecular dynamics simulations, theoretical predictions for the Zimm model and experimental data.

2. Scaling Model

2.1. Dilute Solutions. In dilute solutions the intrachain electrostatic interactions dominate over the interchain ones. These intrachain interactions result in stretching of polyelectrolyte chains. A polyelectrolyte chain can be envisioned as an array of the electrostatic blobs with size D_e and number of monomers g_e . (Here, for simplicity, we will assume Θ -solvent conditions for the polymer backbone. Changing the solvent quality for the polymer backbone will not change dependence of the chain relaxation time on the chain degree of polymerization and polymer concentration.) The statistics of the chain at the length scales smaller than the electrostatic blob size is Gaussian leading to the following relation between the electrostatic blob size D_e , number of monomers in it, g_e , and the fraction of the ionized groups on the polymer backbone f_* .^{2,8,9,12}

$$D_e \approx b(uf_*^2)^{-1/3}, \quad \text{and} \quad g_e \approx (uf_*^2)^{-2/3} \quad (1)$$

where u is the ratio of the Bjerrum length l_B to the bond size b . The Bjerrum length $l_B = e^2/(\epsilon k_B T)$ determines the strength of the electrostatic interactions and is defined as the length scale at which the Coulomb interaction between two elementary charges e , in a dielectric medium with the dielectric constant ϵ , is equal to the thermal energy $k_B T$. In this paper, we will present a scaling analysis of the chain dynamics and will neglect numerical coefficients. The average end-to-end distance of the chain is estimated as the size of the stretched array of electrostatic blobs

$$R_e \approx D_e N/g_e \approx b(uf_*^2)^{1/3} N \quad (2)$$

The fluctuations of the chain size around its average value R_e are on the order of $bN^{1/2}$ and can be neglected for long enough chains. Thus, a polyelectrolyte chain can be viewed as a rodlike polymer of length R_e . (Here we will present a scaling consideration of the chain dynamics which neglects nonuniform chain stretching (see, for details, ref 2).)

A polyelectrolyte chain diffuses a distance on the order of its size during the time interval proportional to the chain relaxation time τ .

$$\langle \Delta R(\tau)^2 \rangle \approx \langle R_e^2 \rangle \approx D\tau \quad (3)$$

For the Rouse dynamics the chain translational friction coefficient is equal to the monomer friction coefficient ξ_0 times the number of monomers on the polymer backbone N , $\xi_N = N\xi_0$. Using the Einstein's relation between the chain's diffusion and friction coefficients, $D = k_B T/(N\xi_0)$, we can evaluate Rouse relaxation time as follows

$$\tau_R \approx \frac{\langle R_e^2 \rangle}{D} \approx \frac{\xi_0 N R_e^2}{k_B T} \approx \tau_0 (uf_*^2)^{2/3} N^3 \quad (4)$$

Thus, this simple calculation shows that in dilute solutions the relaxation time of the Rouse polyelectrolyte chain increases with degree of polymerization, N , as N^3 . Note that the translational relaxation time and the rotational relaxation time have identical scaling dependences on the system parameters.

It is interesting to point out that the Rouse relaxation time of a polyelectrolyte chain is different from the chain's relaxation time in the presence of the hydrodynamic interactions (the so-called Zimm chain's dynamics) by a logarithmic factor. For a rodlike polymer with length R_e and thickness $bN^{1/2}$ the friction coefficient in the presence of the hydrodynamic interactions is on the order of $\xi_Z \approx \xi_0 R_e / (b \ln(R_e/bN^{1/2}))$.⁷ This results in the following expression for the Zimm chain's relaxation time

$$\tau_Z \approx \frac{\tau_0 u f_*^2 N^3}{\ln((u f_*^2)^{1/3} N^{1/2})} \quad (5)$$

Comparing expressions for the Rouse (eq 4) and Zimm (eq 5) relaxation times, one can see that the Zimm relaxation time has slightly stronger dependence on the fraction of ionized groups f_* and value of the interaction parameter u than its Rouse counterpart, but both times have the same leading N dependences (both are proportional to N^3). Note that in the long chain limit the polyelectrolyte with hydrodynamic interactions relaxes faster, $\tau_Z < \tau_R$, due to additional logarithmic factor in the denominator of the eq 5.

In dilute solutions the chain relaxation time decreases with increasing polymer concentration due to counterion condensation, which reduces the fraction of the charged monomers, f_* , on the polymer backbone.

2.2. Semidilute Solutions. In semidilute solution regime the electrostatic interactions are screened at the length scales on the order of the solution correlations length ξ —the average mesh size of the semidilute polyelectrolyte solution.^{2,8,9,12} This is due to the fact that the average charge of the correlation volume ξ^3 is equal to zero because the charge of the section of the chain with g_ξ monomers within the correlation length ξ is compensated by surrounding counterions. The interactions between correlation volumes can be ignored in the zeroth order approximation, and the electrostatic blob size and stretching of a chain can be estimated by taking into account only electrostatic interactions within the correlation volume ξ^3 . The electrostatic interactions

between charged monomers on the length scales smaller than the correlation length result in stretching of the chain sections within correlation blobs. At these length scales a section of polyelectrolyte chain with g_ξ monomer can be viewed as an array of the electrostatic blobs with size $\xi \propto D_e g_\xi / g_e$. The concentration dependence of the number of monomers in a correlation volume ξ^3 can be obtained by imposing the close-packing condition for chain sections of size ξ , $c \approx g_\xi / \xi^3$. The correlation length of semidilute polyelectrolyte solution is estimated as^{2,8,9,12}

$$\xi \approx b(uf_*^2)^{-1/6}(cb^3)^{-1/2} \propto c^{-1/2} \quad (6)$$

This leads to the same concentration dependence of the number of monomers within a correlation volume

$$g_\xi \approx c\xi^3 \approx (uf_*^2)^{-1/2}(cb^3)^{-1/2} \propto c^{-1/2} \quad (7)$$

Since at length scales larger than the correlation length ξ other chains and counterions screen electrostatic interactions, the statistics of the chain are those of a Gaussian chain with the effective persistence length on the order of the correlation length ξ . Thus, according to the scaling model, a chain in the semidilute salt-free polyelectrolyte solution is a random walk of correlation blobs with size^{2,8,9,12}

$$R_c \approx \xi \left(\frac{N}{g_\xi} \right)^{1/2} \approx b(uf_*^2)^{1/12} N^{1/2} (cb^3)^{-1/4} \propto N^{1/2} c^{-1/4} \quad (8)$$

Similar scaling arguments can be applied to describe polymer dynamics. The motion of different chain sections inside the correlation blob are strongly hydrodynamically coupled just as in dilute solutions, leading to the Zimm relaxation time of the correlation blob to be proportional to its volume $\tau_\xi^Z \approx \tau_0 \xi^3$ (up to logarithmic corrections).^{2,8,9,12}

The Rouse model neglects hydrodynamic interactions and predicts the relaxation time of the section of a polyelectrolyte chain with g_ξ monomers inside the correlation blob

$$\tau_\xi^R \approx \tau_0 g_\xi \xi^2 \quad (9)$$

which is the same as the Rouse relaxation time of the polyelectrolyte chain with g_ξ monomers in a dilute solution.

Each chain consists of N/g_ξ correlation blobs. Both electrostatic and hydrodynamic interactions between these blobs are screened and therefore their motion in the unentangled semidilute solution regime can be described by the Rouse dynamics of correlation blobs. In the case of real polyelectrolyte solutions with the Zimm dynamics inside the correlation length, the relaxation time of the chain is^{2,8,9,12}

$$\tau_Z \approx \tau_\xi^Z (N/g_\xi)^2 \approx \tau_0 (uf_*^2)^{1/2} (cb^3)^{-1/2} N^2, \quad c^* < c < c_c \quad (10)$$

Note that the chain relaxation time in this unentangled semidilute regime decreases with increasing polymer concentration as $\tau_Z \sim c^{-1/2}$ because both the number of monomers in the correlation blob g_ξ and the correlation blob size ξ are proportional to $c^{-1/2}$. This decrease of the solution relaxation time with increasing polymer concentration is unique for unentangled polyelectrolyte solutions. Relaxation time of uncharged polymer solutions increases with polymer concentration. The reason for such unusual dependence of polyelectrolyte relaxation time is that

the chain size decreases with increasing polymer concentration while the chain friction coefficient does not change.

In the case of the Rouse polyelectrolyte chain with the chain's dynamics described by the Rouse model on all length scales (neglecting all hydrodynamic interactions) the chain relaxation time has the same dependence on polymer concentration and degree of polymerization as in the case with hydrodynamic interactions inside correlation blob (eq 10)

$$\tau_R \approx \tau_\xi^R (N/g_\xi)^2 \approx \tau_0 (uf_*^2)^{1/6} (cb^3)^{-1/2} N^2, \quad c^* < c < c_c \quad (11)$$

Thus, in semidilute solutions both relaxation time of the Rouse polyelectrolyte chain (see eq 11) and relaxation time of the real polyelectrolyte chain with Zimm dynamics inside the correlation length (see eq 10) decrease as inverse square root of polymer concentration. However, as in dilute solutions, the relaxation time of the real polyelectrolyte chain has stronger dependence on the electrostatic interaction parameter uf_*^2 .

The chain relaxation time can be estimated by monitoring the time correlation function $\langle \mathbf{R}_c(0) \cdot \mathbf{R}_c(t) \rangle$ of the end-to-end vector. At the time scale larger than the relaxation time of the section of the chain inside correlation blob this correlation function is expected to be the sum of the odd Rouse modes⁷

$$\frac{\langle \mathbf{R}_c(0) \mathbf{R}_c(t) \rangle}{\langle \mathbf{R}_c^2 \rangle} = \frac{8}{\pi^2} \sum_{p=1,3,5,\dots} \frac{1}{p^2} \exp\left(-\frac{tp^2}{\tau_R}\right), \quad \text{for } t > \tau_\xi \quad (12)$$

We will use eq 12 to fit correlation function of the end-to-end vector because polymers in our simulations were unentangled in semidilute and concentrated polyelectrolyte solutions. In the next section, we present the results of the tests of the predictions of the scaling model by molecular dynamics simulations.

3. Molecular Dynamics Simulations of Polyelectrolyte Solution Dynamics

3.1. Model and Methodology.^{29–31} A polyelectrolyte solution was represented in our simulations by an ensemble of $M = 16$ chains each consisting of N Lennard-Jones (LJ) monomers, with fraction f of charged monomers and $N_c = fN$ counterions per chain confined into a cubic simulation box of size L_C with periodic boundary conditions. We have considered fully and partially charged polyelectrolyte chains with fraction of charged monomers $f = 1$ and $f = 1/2$ respectively. All charged particles were monovalent ions and, therefore, the total number of charged monomers was equal to the number of counterions MN_c . Excluded volume interactions between every pair of monomers were modeled by the truncated-shifted Lennard-Jones (LJ) potential set to zero at the cutoff distance $r_c = 2.5\sigma$.

$$U_{LJ}(r) = \begin{cases} 4\epsilon_{LJ} \left[\left(\frac{\sigma}{r} \right)^{12} - \left(\frac{\sigma}{r} \right)^6 - \left(\frac{\sigma}{r_c} \right)^{12} + \left(\frac{\sigma}{r_c} \right)^6 \right] & r \leq r_c \\ 0 & r > r_c \end{cases} \quad (13)$$

The parameter ϵ_{LJ} controls the strength of the short-range interactions. All simulations were carried out for $\epsilon_{LJ} = 1.5 k_B T$ (k_B is the Boltzmann constant and T is the absolute temperature), which corresponds to the poor solvent condition for the uncharged backbone. For many synthetic polyelectrolytes such as NaPSS water is a poor solvent for the polymer backbone. It is also important to point out that for highly charged chains the solvent quality for the polymer backbone does not have a strong effect on solution properties.^{29–30}

The connectivity of monomers in the chains was maintained by the finite extension nonlinear elastic (FENE) potential

$$U_{\text{FENE}}(r) = -\frac{1}{2} k R_0^2 \ln\left(1 - \frac{r^2}{R_0^2}\right) \quad (14)$$

where $k = 7\epsilon_{\text{LJ}}/\sigma^2$ is the spring constant and $R_0 = 2\sigma$ is the maximum bond length at which the elastic energy of the bond becomes infinite. The FENE potential gives only the attractive part of the bond potential. The values of the parameters were chosen to prevent chains from crossing each other.

A truncated-shifted Lennard-Jones potential was also used to describe the pure repulsive excluded volume interactions between any pair of counterions and between a monomer and a counterion.

$$U_{\text{LJ}}^{\text{S}}(r) = \begin{cases} 4\epsilon_{\text{LJ}}\left[\left(\frac{\sigma}{r}\right)^{12} - \left(\frac{\sigma}{r}\right)^6\right] + \epsilon_{\text{LJ}} & r \leq 2^{1/6}\sigma \\ 0 & r > 2^{1/6}\sigma \end{cases} \quad (15)$$

The parameter σ was chosen to be the same for all monomers and counterions.

The solvent was represented by a continuum with the dielectric constant ϵ . In such effective medium representation of the solvent, all charged particles interact with each other via the unscreened Coulomb potential

$$U_{\text{Coul}}(r) = k_{\text{B}}T \frac{l_{\text{B}}q_iq_j}{r} \quad (16)$$

where $l_{\text{B}} = e^2/(\epsilon k_{\text{B}}T)$ is the Bjerrum length, q_i is the charge valence of the i th particle equal to $+1$ for a positive charge and -1 for a negative charge. The electrostatic interactions between all charges in the simulation box and all their periodic images were computed by the smoothed particle mesh Ewald (SPME) algorithm^{36–38} implemented in the DL_POLY version 2.12 software package.

The molecular dynamics (MD) simulations were performed by the following procedure.^{29–31} The initial conformations of the 16 polyelectrolyte chains in the cubic cell with periodic boundary conditions were generated as a set of self-avoiding walks. The counterions were placed randomly in the unoccupied volume of the simulation box. Both dilute and semidilute solutions of chains with the degree of polymerization N varying from 25 to 373 and the value of the Bjerrum length $l_{\text{B}} = 3\sigma$, were studied in the range of polymer concentrations c from $1.5 \times 10^{-7} \sigma^{-3}$ to $0.15 \sigma^{-3}$. The simulations were carried out at constant temperature $T = 2\epsilon_{\text{LJ}}/(3k_{\text{B}})$ using the Langevin thermostat with a coupling constant $z = 0.1414m/\tau_{\text{LJ}}$, where m is a particle mass (set in our simulations to unity) and τ_{LJ} is the characteristic LJ-time defined as $\tau_{\text{LJ}} = \sqrt{m\sigma^2/k_{\text{B}}T}$. Utilization of the Langevin thermostat in our simulations corresponds to the Rouse chain dynamics. A velocity Verlet algorithm was used to integrate the equations of motion with a time step equal to $\Delta t = 0.01\tau_{\text{LJ}}$. The number of MD steps was chosen large enough to allow the mean square end-to-end distances and the mean square radii of gyration of chains to relax to their equilibrium values. This requirement led to the range of simulation runs between 200 000 and 8 000 000 MD steps depending on the chain length and polymer concentration.

3.2. Results and Discussion. The chain relaxation time in our simulations was estimated by monitoring both the decay of the correlations in the orientation of the end-to-end vector (see eq 12) and the time dependence of the mean-square displacement of the chain center of mass. Figure 1 shows the time evolution

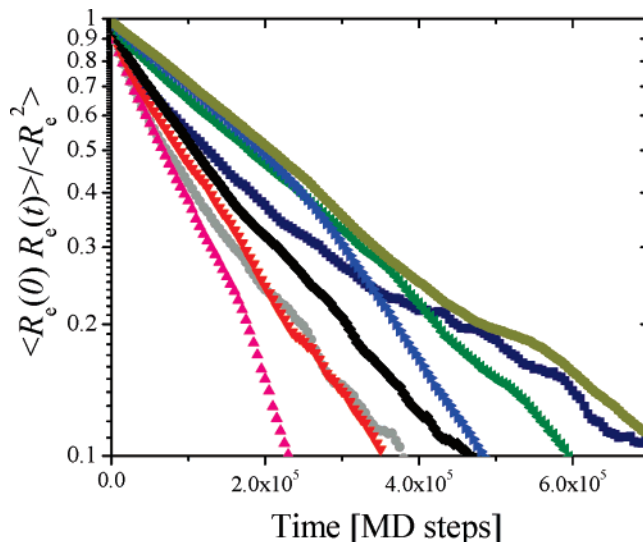


Figure 1. Orientation correlation function of the end-to-end vector for the system of fully charged chains, $f = 1$, with the degree of polymerization $N = 94$ at different polymer concentrations: $1.5 \times 10^{-6} \sigma^{-3}$ (olive green hexagons); $1.5 \times 10^{-5} \sigma^{-3}$ (blue triangles); $1.5 \times 10^{-4} \sigma^{-3}$ (green triangles); $1.5 \times 10^{-3} \sigma^{-3}$ (black rhombs); $0.005 \sigma^{-3}$ (red triangles); $0.015 \sigma^{-3}$ (pink triangles); $0.05 \sigma^{-3}$ (gray circles); $0.15 \sigma^{-3}$ (dark blue squares).

of the end-to-end vector correlation function during the simulation runs of the systems of fully charged chains, $f = 1$, with the degree of polymerization $N = 94$. The chain relaxation time was evaluated by fitting the simulation data to the correlation function given by eq 12. The obtained correlation times of end-to-end vectors show identical N and concentration dependences as the diffusion times estimated from the mean-square displacement of the chain center of mass.

Parts a and b of Figure 2 show the N dependence of the end-to-end vector relaxation time at different polymer concentrations for fully, $f = 1$, and partially, $f = 1/2$, charged chains. In a dilute solution regime the data points approach N^3 dependence while in semidilute solution regime the data are closer to N^2 dependence. The crossover between the two N dependence regimes occurs around chain overlap concentration c^* . These N dependences of the chain relaxation time are in an agreement with the predictions of the scaling model described in section 2.

Our simulations confirm theoretical predictions that relaxation time in polyelectrolyte solution decreases with polymer concentration in both dilute and semidilute regimes as seen in Figure 3, parts a and b. In the dilute solution regime, the chain relaxation time shows weak concentration dependence. In this concentration interval, the decrease of the chain relaxation time is caused by the chain size reduction due to counterion condensation on the polymer backbone. With increasing polymer concentration, the entropic penalty for counterion localization decreases, resulting in a larger number of counterions residing in the vicinity of the polymer backbone. These counterions weaken intrachain electrostatic repulsion and reduce the polymeric size.

In the semidilute solution regime, the chain relaxation time first decreases with increasing polymer concentration then it begins to increase. The size of the correlation blob decreases with increasing polymer concentration leading to weaker intrachain electrostatic interaction which are screened by surrounding counterions. To verify the scaling relations derived in section 2, we replotted the simulation data corresponding to the semidilute solution regime using the following universal

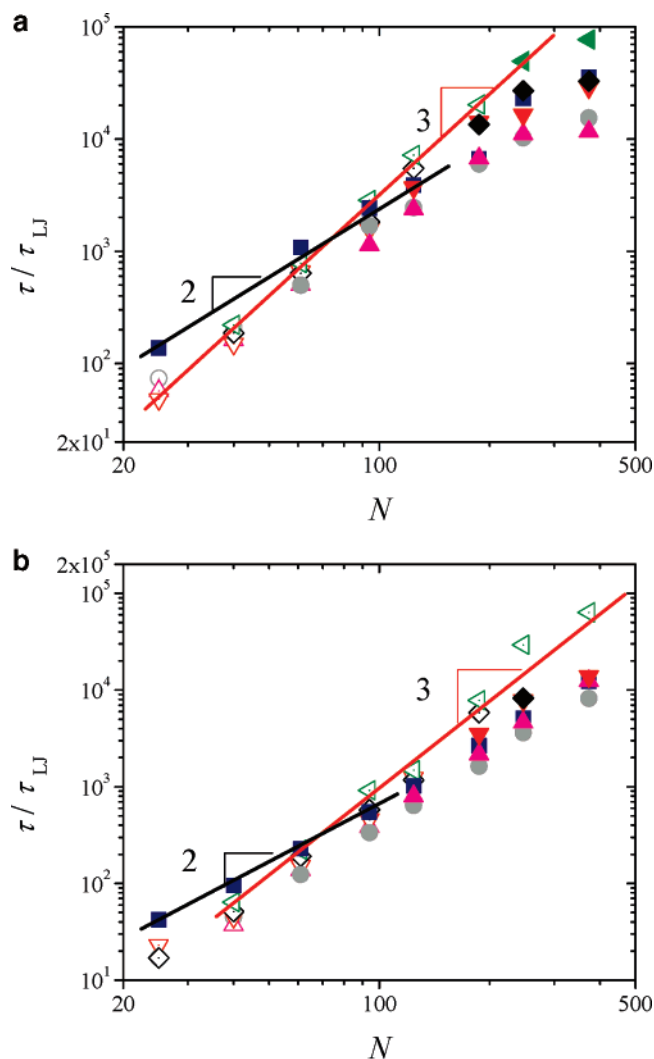


Figure 2. Dependence of the chain relaxation time on the chain degree of polymerization at different polymer concentrations: $1.5 \times 10^{-4} \sigma^{-3}$ (green triangles); $1.5 \times 10^{-3} \sigma^{-3}$ (black rhombs); $0.005 \sigma^{-3}$ (red triangles); $0.015 \sigma^{-3}$ (pink triangles); $0.05 \sigma^{-3}$ (gray circles); $0.15 \sigma^{-3}$ (dark blue squares) for the system of fully (a) and partially (b) charged chains. Open symbols correspond to dilute and filled symbols to semidilute solution regimes.

coordinates $\tau/(N\xi)^2$ vs c (see Figure 4, parts a and b). All simulation data collapsed into one universal curve. At the intermediate polymer concentration range the simulation data follow $c^{1/2}$ scaling in an agreement with theoretical predictions for the Rouse chain dynamics, $\tau/(N\xi)^2 \sim c^{1/2}$. However, at high polymer concentrations, $c > 0.015$ for $f = 1$ and $c > 0.05$ for $f = 1/2$, the simulation data exhibit faster than $c^{1/2}$ increase with polymer concentration. In the case of the fully charged chains, the simulation data scale almost linearly with polymer concentration.

The crossover to the new concentration regime is independent of the degree of polymerization. Thus, it cannot be associated with the entanglement threshold. The absence of the N dependence of the crossover concentration leaves us with two possible explanations of the slowdown of the chain dynamics. The upturn in the chain relaxation time could be due to the crossover to concentrated solution regime in which the electrostatic interactions between charged monomers are completely screened and chain dynamics is similar to that of neutral chains. The crossover to the concentrated solution regime² occurs at $c = c_b$. The second possibility is that the system approaches a glass transition with increasing polymer concentration which

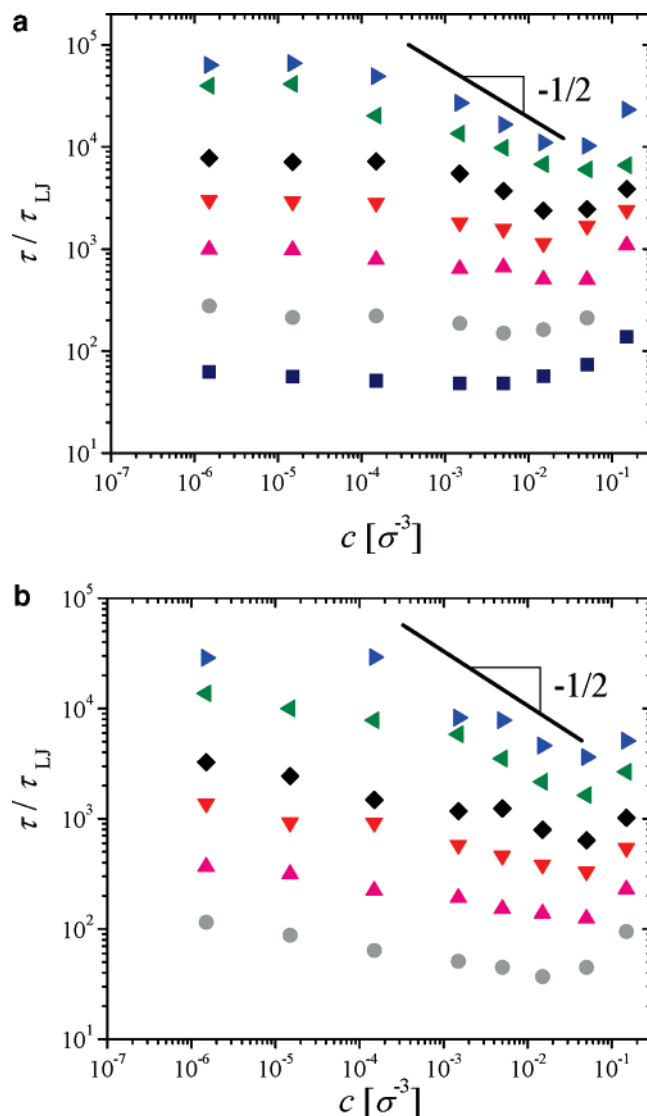


Figure 3. Concentration dependence of the chain relaxation time for the system of fully (a) and partially (b) charged chains. $N = 25$ (dark blue squares); $N = 40$ (gray circles); $N = 64$ (pink triangles); $N = 94$ (red triangles); $N = 124$ (black rhombs); $N = 187$ (green triangles); $N = 247$ (blue triangles).

is manifested in an increase of the effective monomeric friction coefficient. We can dismiss the first explanation because if it was the case the crossover to the concentrated solution regime should occur at lower polymer concentrations for the system of partially charged chains, $c_b \sim f^{2/3}$.^{2,8,9} This is not observed in our simulations. The crossover to the new concentration regime occurs at higher polymer concentration for the partially charged chains $f = 1/2$ than for the fully charged ones. Thus, we can argue that the upturn in the chain relaxation time is due to the increase of the effective monomeric friction coefficient with increasing polymer concentration.³⁹ For solutions of fully charged chains, $f = 1$, the total concentration of counterions and monomers is equal to twice the polymer concentration. This makes average distance between charges shorter and electrostatic interactions stronger in comparison with the system of partially charged chains, $f = 1/2$, and therefore, the transition occurs earlier for fully charged chains.

In order to directly test the hypothesis of the concentration dependence of the monomeric friction coefficient we have studied the concentration dependence of the chain diffusion coefficient D . Note that, for the Rouse model the chain diffusion coefficient is inversely proportional to the chain degree of

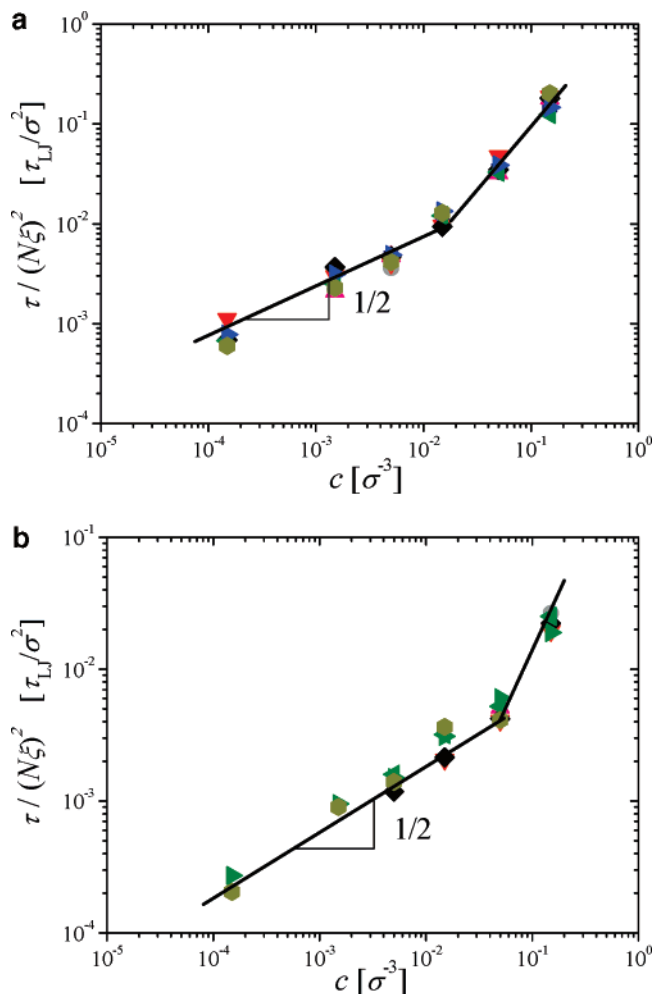


Figure 4. Verification of the scaling relations in semidilute solution regime for the system of fully (a) and partially (b) charged chains.

polymerization N times the monomeric friction coefficient ξ_0 , $D = k_B T / (N\xi_0)$. The results of this study are shown in Figure 5, parts a and b. The chain diffusion coefficient D monotonically decreases with polymer concentration. This decrease is almost unnoticeable at very low concentrations ($c < 10^{-4} \sigma^{-3}$). However, chain diffusion coefficient shows strong concentration dependence at higher polymer concentrations ($c > 10^{-3} \sigma^{-3}$). It is interesting to point out that the simulation results can be fitted to the exponential function $DN = D_0 \exp(-B(2fc b^3)^{1/3})$ over almost entire concentration range. The parameter B is equal to 2.56 for both fractions of charged monomers and the parameter D_0 is equal to $4.33 \sigma^2/\tau_{LJ}$ for the fully charged chains, $f = 1$, and $5.67 \sigma^2/\tau_{LJ}$ for the partially charged chains, $f = 1/2$ (see solid lines in Figure 5).

The renormalization of the monomeric friction coefficient can be included into the Rouse model by substituting the characteristic monomeric time τ_0 by the effective monomeric time $\tau_{\text{eff}} = \sigma^2/(DN)$ which takes into account the variation of the monomeric friction coefficient with polymer concentration.

$$\tau_R \approx \tau_{\text{eff}}(uf_*^2)^{1/6} N^2 (cb^3)^{-1/2}, c^* < c < c_e \quad (17)$$

To test this hypothesis, in Figure 6, parts a and b, we plot the dependence of the reduced chain relaxation time $\tau/(\tau_{\text{eff}} g_\xi \xi_0^2)$ on the number of correlation blobs per chain N/g_ξ . This plot confirms that our data in the concentration range above c^*

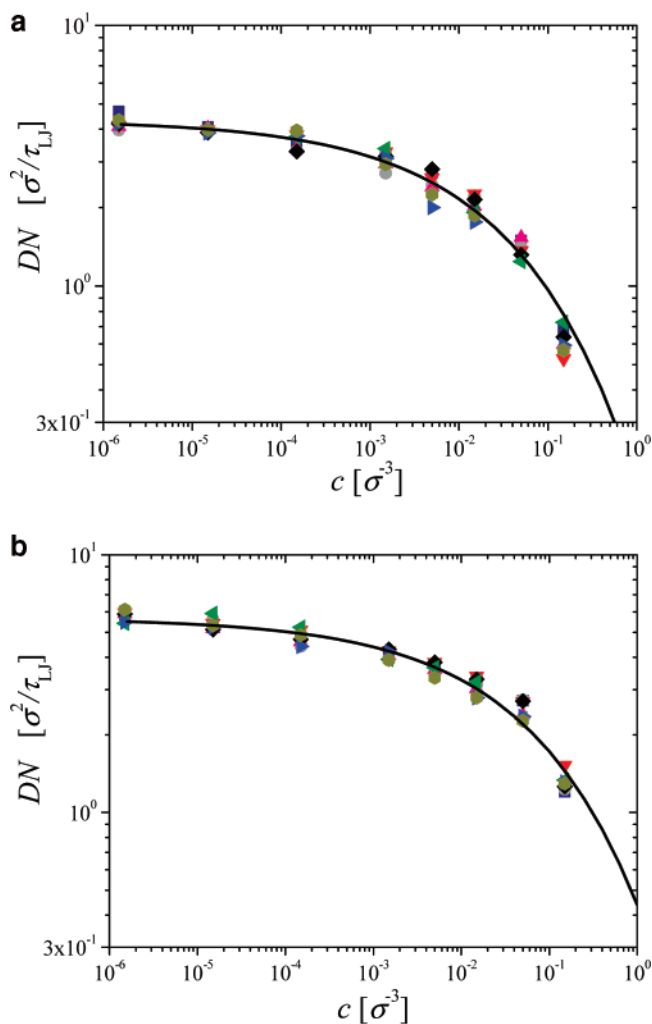


Figure 5. Dependence of the product of the chain diffusion coefficient and chain degree of polymerization N , DN on the polymer concentration for the system of fully (a) and partially (b) charged chains. $N = 25$ (dark blue black squares); $N = 40$ (gray circles); $N = 64$ (pink triangles); $N = 94$ (red triangles); $N = 124$ (black rhombs); $N = 187$ (green triangles); $N = 247$ (blue triangles); $N = 373$ (olive green hexagons).

follows the Rouse dynamics with concentration dependent monomeric friction coefficient.

$$\tau_R \approx \tau_{\text{eff}} g_\xi \xi_0^2 b^{-2} \left(\frac{N}{g_\xi} \right)^2, c^* < c < c_e \quad (18)$$

It is important to point out that the strong renormalization of the monomeric friction coefficient could be a unique feature of the simulations without explicit solvent. The simulations with explicit solvent could show much weaker concentration dependence of the monomeric friction coefficient.

Until now we have presented a detailed study of the whole chain dynamics. It is interesting to see how well the Rouse model describes the dynamic properties of the polyelectrolyte chains at shorter length and time scales. To achieve this goal we studied behavior of the amplitudes of the Rouse modes $\mathbf{X}_p(t)$ defined as the cosine transform of the radius vector $\mathbf{r}_n(t)$ of the n th monomer on the polymer backbone⁷

$$\mathbf{X}_p(t) = \frac{1}{N} \int_0^N dn \mathbf{r}_n(t) \cos\left(\frac{\pi p n}{N}\right) \quad (19)$$

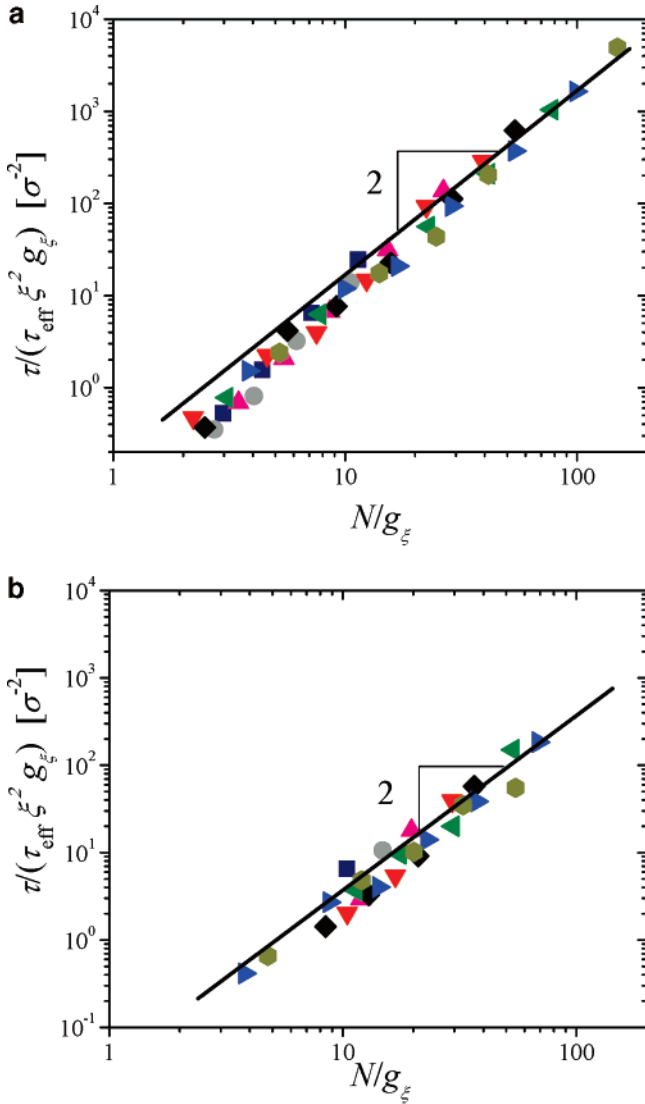


Figure 6. Dependence of the reduced chain relaxation time $\tau/(\tau_{\text{eff}}\xi^2g_\xi)$ on the number of correlation blobs N/g_ξ per chain for the system of fully (a) and partially (b) charged chains. $N = 25$ (dark blue black squares); $N = 40$ (gray circles); $N = 64$ (pink triangles); $N = 94$ (red triangles); $N = 124$ (black rhombs); $N = 187$ (green triangles); $N = 247$ (blue triangles); $N = 373$ (olive green hexagons).

In dilute polyelectrolyte solutions the strong intrachain electrostatic interactions result in elongation of the polyelectrolyte chain. In this concentration regime the average mean-square distance between n th and m th monomers on the polymer backbone is equal to

$$\langle(\mathbf{r}_n(t) - \mathbf{r}_m(t))^2\rangle \approx \frac{D_e^2}{g_e^2}(n - m)^2 + b|n - m|, \quad c < c^* \quad (20)$$

where the first term in the rhs of the eq 20 describes an elongation of the polyelectrolyte chain into array of the electrostatic blobs and the second term describes chain fluctuations around this rodlike conformation. In semidilute solution regime for the length scales shorter than solution correlation length ξ , the chain statistics is similar to the one in the dilute solution regime. Thus, eq 20 can be used to describe mean-square average distance between two monomers for which the distance along the polymer backbone $|n - m|$ is smaller than the number of monomers in the correlation blob g_ξ . At the larger

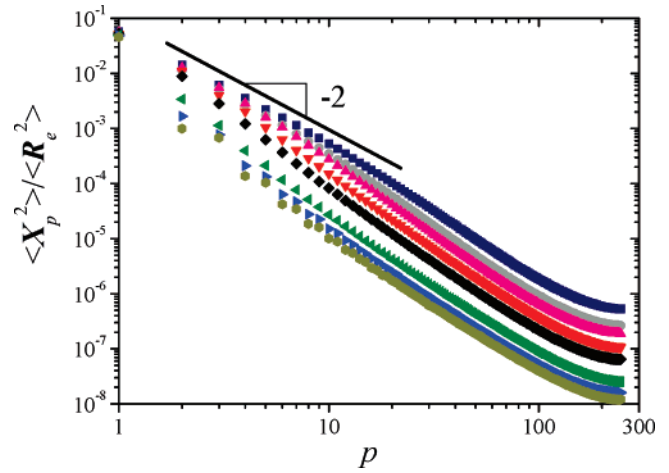


Figure 7. Dependence of the reduced mean-square average value of the Rouse mode amplitudes on the mode number p for fully charged chains with the degree of polymerization $N = 247$ at different polymer concentrations: $1.5 \times 10^{-6} \sigma^{-3}$ (olive green hexagons); $1.5 \times 10^{-5} \sigma^{-3}$ (blue triangles); $1.5 \times 10^{-4} \sigma^{-3}$ (green triangles); $1.5 \times 10^{-3} \sigma^{-3}$ (black rhombs); $0.005 \sigma^{-3}$ (red triangles); $0.015 \sigma^{-3}$ (pink triangles); $0.05 \sigma^{-3}$ (gray circles); $0.15 \sigma^{-3}$ (dark blue squares).

length scale for the distances along polymer backbone $|n - m| > g_\xi$ the electrostatic interactions are screened and a polyelectrolyte chain behaves as an ideal chain with the Kuhn length on the order of the solution correlation length ξ with the average mean-square distance between n th and m th monomers being equal to

$$\langle(\mathbf{r}_n(t) - \mathbf{r}_m(t))^2\rangle \approx \frac{\xi^2}{g_\xi^2}|n - m|, \quad |n - m| > g_\xi \text{ and } c > c^* \quad (21)$$

Using expressions in eqs 20 and 21, we can calculate the mean-square average value of the Rouse mode amplitudes in dilute and semidilute solution regimes (see, for details, ref 7)

$$\langle\mathbf{X}_p^2(t)\rangle \approx \begin{cases} \langle R_e^2 \rangle \frac{\sin^4(\pi p/2)}{(\pi p)^4} + \frac{b^2 N}{(\pi p)^2}, & \text{for } c < c^* \\ N^2 \frac{D_e^2 \sin^2\left(\frac{\pi p g_\xi}{N}\right)}{g_e^2 (\pi p)^3} + \frac{b^2 N}{(\pi p)^2}, & \text{for } c^* < c \end{cases} \quad (22)$$

It follows from eq 22 that in a dilute solution there is an even-odd mode effect. For even modes with $p = 2, 4, 6, \dots$, the first term is exactly zero and the mode spectrum is identical to the spectrum of the Rouse modes of an ideal polymer chain. However, for the odd modes with $p = 1, 3, 5, \dots$, the mode spectrum is dominated by the first term for low-frequency modes. Thus, one should expect oscillations in the mode spectrum with magnitude of oscillations decaying with increasing the mode number p . Figure 7 shows the spectrum of the Rouse modes for the fully charged polyelectrolyte chain with the degree of polymerization $N = 247$. To obtain this spectrum from our simulations we have used the discrete Fourier transform of the monomer coordinates

$$\mathbf{X}_p(t) = \frac{1}{N} \sum_{n=0}^{N-1} \mathbf{r}_n(t) \cos\left(\frac{\pi p(n + 1/2)}{N}\right) \quad (23)$$

As one can see in a dilute solution regime, there are indeed oscillations in the mode spectrum in agreement with eq 22, c

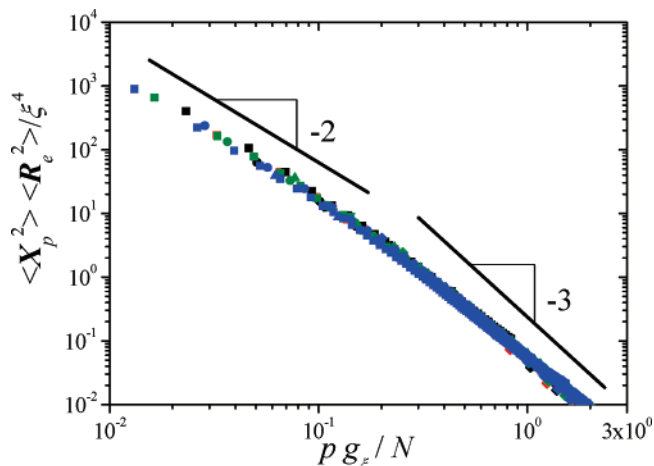


Figure 8. Universal plot $\langle \mathbf{X}_p^2(t) \rangle \langle R_e^2 \rangle / \xi^4$ vs pg_ξ / N for the systems of fully charged chains, $f = 1$, with the degree of polymerizations $N = 94$ (red symbols), 124 (black symbols), 187 (green symbols) and 247 (blue symbols) in semidilute solution regime at different polymer concentrations: $1.5 \times 10^{-3} \sigma^{-3}$ (rhombs); $0.005 \sigma^{-3}$ (inverted triangles); $0.015 \sigma^{-3}$ (triangles); $0.05 \sigma^{-3}$ (circles); $0.15 \sigma^{-3}$ (blue squares).

$< c^*$. In the semidilute solution regime $\langle \mathbf{X}_p^2(t) \rangle$ approaches p^{-2} asymptotic in agreement with the $pg_\xi / N \ll 1$ limit of eq 22.

Analysis of the mode spectrum in semidilute solution regime, $c > c^*$,

$$\langle \mathbf{X}_p^2(t) \rangle \approx \frac{g_\xi^3 D_e^2 \sin\left(\frac{\pi p g_\xi}{N}\right)}{N g_e^2 (\pi p g_\xi / N)^3} + \frac{b^2 g_\xi^2}{N (\pi p g_\xi / N)^2} \approx \frac{\xi^4 \sin\left(\frac{\pi p g_\xi}{N}\right)}{\langle R_e^2 \rangle (\pi p g_\xi / N)^3} \quad (24)$$

shows that one can select universal coordinates $\langle \mathbf{X}_p^2(t) \rangle \langle R_e^2 \rangle / \xi^4$ and pg_ξ / N that eliminate an N dependence and collapse simulation data for different chain degrees of polymerizations and different polymer concentrations onto one universal plot. (Note that in rewriting eq 24 we have used the following relations $\xi \approx D_e g_\xi / g_e$ and $\langle R_e^2 \rangle \approx \xi^2 N / g_\xi$, neglected the second term because it is small for $D_e \ll \xi$.) This universal scaling plot is presented in Figure 8. There are two clear asymptotic regimes in Figure 8. For small values of the normalized mode number, $pg_\xi / N \ll 1$, the function $\langle \mathbf{X}_p^2(t) \rangle \langle R_e^2 \rangle / \xi^4$ is proportional to p^{-2} while for the mode numbers with $pg_\xi / N \sim 1$, it scales with the mode number p as p^{-3} . This is exactly what one should expect in accordance with eq 24.

The mode relaxation time τ_p can be obtained from the time correlation function of the Rouse mode amplitudes, $\langle \mathbf{X}_p(t) \cdot \mathbf{X}_p(t + \Delta t) \rangle$. In analysis of our simulation data we have fitted the correlation function to a simple exponential function of the following form

$$\langle \mathbf{X}_p(t) \cdot \mathbf{X}_p(t + \Delta t) \rangle = \langle \mathbf{X}_p^2(t) \rangle \exp(-\Delta t / \tau_p) \quad (25)$$

In the framework of the preaveraging approximation⁷ the relaxation times of the Rouse modes τ_p are proportional to the mode friction coefficient ζ_p and $\langle \mathbf{X}_p^2(t) \rangle$, $\tau_p \propto \zeta_p \langle \mathbf{X}_p^2(t) \rangle$. In this approximation, the effect of the electrostatic interactions is included into renormalization of the parameters ζ_p and $\langle \mathbf{X}_p^2(t) \rangle$. In order to test the validity of this approximation for polyelectrolyte solutions, we have plotted the dependence of the reduced mode relaxation time $\tau_p / (\tau_{\text{eff}} \xi^2 g_\xi^2)$ on the reduced mode number pg_ξ / N in Figure 9. Normalization of the mode

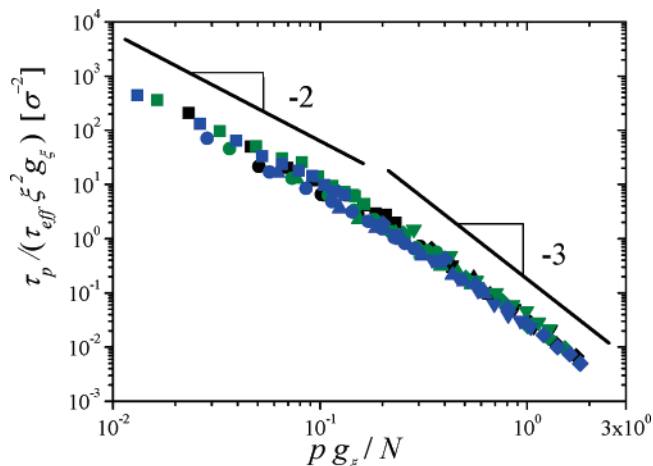


Figure 9. Dependence of the reduced mode relaxation time $\tau_p / (\tau_{\text{eff}} \xi^2 g_\xi^2)$ on the reduced mode number pg_ξ / N for the systems of the fully charged chains, $f = 1$, with the degree of polymerizations 124 (black), 187 (green), and 247 (blue) in semidilute solution regime at different polymer concentrations: $1.5 \times 10^{-3} \sigma^{-3}$ (rhombs), $0.005 \sigma^{-3}$ (inverted triangles), $0.015 \sigma^{-3}$ (triangles), $0.05 \sigma^{-3}$ (circles), and $0.15 \sigma^{-3}$ (squares).

relaxation time τ_p by τ_{eff} allowed us to account for renormalization of the mode friction coefficient with increasing polymer concentration. There are two different scaling regimes in Figure 9. For small values of the parameter pg_ξ / N the reduced mode relaxation time decreases with increasing the mode number p as p^{-2} . These Rouse modes correspond to relaxation processes occurring on the length scales larger than solution correlation length ξ . For these length scales, the electrostatic interactions are screened and chain dynamics is similar to the dynamics of the ideal chain with the Kuhn length on the order of the solution correlation length ξ . For modes with shorter wavelength, $pg_\xi / N \sim 1$, the reduced chain relaxation time shows faster decrease with the mode number p , $\tau_p \sim p^{-3}$ (see also eq 24). This faster decay of the mode relaxation time τ_p with the mode number p corresponds to relaxation processes of the sections of the chain smaller than the solution correlation length ξ . Note that this dependence of the mode relaxation time, $\tau_p \sim p^{-3}$, on the mode number p is a reflection of the strong elongation of the polyelectrolyte chain at these length scales. Thus, the analysis of the modes amplitudes (Figure 8) and the spectrum of the mode relaxation times (Figure 9) confirms the validity of the preaveraging approximations for polyelectrolyte solutions, and the existence of the single correlation length ξ , which describes both static and dynamics properties of the semidilute polyelectrolyte solutions.

4. Summary

We have performed molecular dynamics simulations of polyelectrolyte dynamics in dilute and semidilute solutions regimes. In our simulations we used Langevin thermostat to control system temperature. The simulations with the Langevin thermostat correspond to the fully draining (Rouse) dynamics of polymer chains for which the effective chain friction coefficient is proportional to the number of monomers on the polymer backbone N . Our simulations have shown that in the dilute solution regime the chain relaxation time scales with the chain degree of polymerization as N^3 . This strong N dependence of the chain relaxation time is a manifestation of the strong elongation of a polyelectrolyte chain due to intrachain electrostatic interactions. The chain relaxation time decreases with increasing polymer concentration. The decrease in the chain

relaxation time in dilute solutions can be explained by chain contraction due to counterion condensation. As polymer concentration increases, the entropic penalty for counterion localization near the polymer backbone decreases leading to the larger fraction of the counterions residing in the vicinity of the polymer chain. The increase in the number of condensed counterions weakens the electrostatic coupling between sections of the polymer chain decreasing polymer size and speeding up its motion.

In semidilute solution regime, we observed the inverse square-root dependence of the chain relaxation time on the polymer concentration, $\tau \sim c^{-1/2}$. In this concentration regime the electrostatic interactions are screened at the length scales on the order of the solution correlation length ξ . Thus, a polyelectrolyte chain can be considered as a Rouse chain of correlation blobs. However, at the length scales smaller than the solution correlation length the strong electrostatic coupling between sections of the chain still persists and determines the characteristic relaxation time of these chain's sections. This dependence of the chain relaxation time is in a good qualitatively agreement with the experimental data by Colby's group^{14,15,21,23} on the variety of the polyelectrolyte systems and is the main reason behind the famous Fuoss law for the concentration dependence of the polyelectrolyte solution viscosity.

The crossover to the new concentration regime, where chain relaxation time increases with polymer concentration, occurs at $c > 0.015$ for fully charged, $f = 1$, and at $c > 0.05$ for partially charged, $f = 1/2$, polyelectrolyte chains. The crossover concentrations are independent of the chain's degree of polymerization. Thus, this increase in the chain relaxation time cannot be related to the crossover to the entangled solution regime.^{2,14,15,21,23} In fact, it is due to the increase of the monomeric friction coefficient with increasing polymer concentration. It is possible that the upturn in the solution viscosity observed in the Boris and Colby experiments²¹ and thought as the crossover to the entangled solution regime is in part due to the renormalization of the monomeric friction coefficient since it shows unexpectedly weak N dependence, $c_e \sim N^{-0.6}$. Our simulations also show that the unentangled semidilute solution regime is very wide. The longest chains with $N = 373$ and 247 start to overlap at about $10^{-4} \sigma^{-3}$ and do not show any effect of entanglements up to our highest polymer concentration $0.15 \sigma^{-3}$. Thus, the unentangled semidilute solution regime spans 3 decades above the overlap concentration. This result is in agreement with the prediction of the scaling model of polyelectrolyte solutions.^{2,8,9}

Acknowledgment. The authors are grateful to the National Science Foundation for financial support under Grants CHE-0616925 and CTS-0609087, the National Institutes of Health under Grant 1-R01-HL0775486A, NASA under Agreement NCC-1-02037 (M.R.), and the donors of the Petroleum Research Fund, administered by the American Chemical Society, for the support of this research under Grant PRF#44861-AC7 (A.V.D.). Q.L. has received the financial support for this work from the

National Natural Science Foundation of China under Grants 20474075 and 20674091.

References and Notes

- (1) Barrat, J.-L.; Joanny, J.-F. *Adv. Chem. Phys.* **1996**, *94*, 1.
- (2) Dobrynin, A. V.; Rubinstein, M. *Prog. Polym. Sci.* **2005**, *30*, 1049.
- (3) Mandel, M. *Encyclopedia of Polymer Science and Engineering*; Wiley: New York, 1988.
- (4) Oosawa, F. *Polyelectrolytes*; Marcel Dekker: New York, 1971.
- (5) Levin, Y. *Rep. Prog. Phys.* **2002**, *65*, 1577.
- (6) Holm, C.; et al. *Adv. Polym. Sci.* **2004**, *166*, 67.
- (7) Doi, M.; Edwards, S. F. *The theory of polymer dynamics*; Clarendon Press: Oxford, U.K., 1989.
- (8) Dobrynin, A. V.; Colby, R. H.; Rubinstein, M. *Macromolecules* **1995**, *28*, 1859.
- (9) Rubinstein, M.; Colby, R. H.; Dobrynin, A. V. *Phys. Rev. Lett.* **1994**, *73*, 2776.
- (10) Muthukumar, M. *J. Chem. Phys.* **1997**, *107*, 2619.
- (11) Muthukumar, M. *J. Chem. Phys.* **1996**, *105*, 5183.
- (12) de Gennes, P.-G.; Pincus, P.; Brochard, F.; Velasco, R. M. *J. Phys. (Fr.)* **1976**, *37*, 1461.
- (13) Cong, R. J.; Temyanko, E.; Russo, P. S.; Edwin, N.; Uppu, R. M. *Macromolecules* **2006**, *39*, 731.
- (14) Krause, W. E.; Tan, J. S.; Colby, R. H. *J. Polym. Sci., Part B: Polym. Phys.* **1999**, *37*, 3429.
- (15) Krause, W. E.; Bellomo, E. G.; Colby, R. H. *Biomacromolecules* **2001**, *2*, 65.
- (16) Lauten, R. A.; Nystrom, B. *Macromol. Chem. Phys.* **2000**, *201*, 677.
- (17) Liu, H.; et al. *J. Chem. Phys.* **1998**, *109*, 7556.
- (18) Pabon, M.; Selb, J.; Candau, F. *Langmuir* **1998**, *14*, 735.
- (19) Pecora, R. *Macromol. Symp.* **2005**, *229*, 18.
- (20) Pristinski, D.; Kozlovskaya, V.; Sukhishvili, S. A. *J. Chem. Phys.* **2005**, *122*.
- (21) Boris, D. C.; Colby, R. H. *Macromolecules* **1998**, *31*, 5746.
- (22) Morawetz, H. *J. Polym. Sci., Part B: Polym. Phys.* **2002**, *40*, 1080.
- (23) Dou, S.; Colby, R. J. *Polym. Phys., Part B: Polym. Phys.* **2006**, *44*, 2001.
- (24) Dobrynin, A. V.; Rubinstein, M.; Obukhov, S. P. *Macromolecules* **1996**, *29*, 2974.
- (25) Dobrynin, A. V. In *Simulation Methods for Polymers*; Kotelyanskii, M., Theodorou, D. N., Eds.; Marcel Dekker: New York, 2004; pp 259–312.
- (26) Limbach, H. J.; Holm, C. *Comput. Phys. Commun.* **2002**, *147*, 321.
- (27) Limbach, H. J.; Holm, C.; Kremer, K. *Macromol. Symp.* **2004**, *211*, 43.
- (28) Micka, U.; Holm, C.; Kremer, K. *Langmuir* **1999**, *15*, 4033.
- (29) Liao, Q.; Dobrynin, A. V.; Rubinstein, M. *Macromolecules* **2006**, *39*, 1920.
- (30) Liao, Q.; Dobrynin, A. V.; Rubinstein, M. *Macromolecules* **2003**, *36*, 3386.
- (31) Liao, Q.; Dobrynin, A. V.; Rubinstein, M. *Macromolecules* **2003**, *36*, 3399.
- (32) *Multilayer Thin Films*; Wiley-VCH: New York, 2003.
- (33) Grosberg, A. Y.; Nguyen, T. T.; Shklovskii, B. I. *Rev. Mod. Phys.* **2002**, *74*, 329.
- (34) Rubinstein, M.; Colby, R. *Polymer Physics*; Oxford University Press: New York, 2003.
- (35) Grosberg, A. Y.; Khokhlov, A. R. *Statistical Physics of Macromolecules*; AIP Press: New York, 1994.
- (36) Rapaport, D. C. *The Art of Molecular Dynamics Simulation*; Cambridge University Press: New York, 1995.
- (37) Essmann, U.; et al. *J. Chem. Phys.* **1995**, *103*, 8577.
- (38) Frenkel, D.; Smit, B. *Understanding Molecular Simulations*; Academic Press: San Diego, CA, 2001.
- (39) Debenedetti, P. G. *Metastable Liquids. Concepts and Principles*; Princeton University Press: Princeton, NJ, 1996.

MA070666E